Acta Biomaterialia 7 (2011) 3027–3035

Contents lists available at ScienceDirect

Acta Biomaterialia

journal homepage: www.elsevier.com/locate/actabiomat

Endothelial cells guided by immobilized gradients of vascular endothelial growth factor on porous collagen scaffolds

Devang Odedra [a,b], Loraine L.Y. Chiu [b], Molly Shoichet [a,b,c,d,*], Milica Radisic [a,b,e,*]

[a] Institute of Biomaterials and Biomedical Engineering, University of Toronto, Toronto, Ontario, Canada
[b] Department of Chemical Engineering and Applied Chemistry, University of Toronto, Toronto, Ontario, Canada M5S 3G9
[c] Department of Chemistry, University of Toronto, Toronto, Ontario, Canada
[d] Terrence Donnelly Centre for Cellular and Biomolecular Research, Toronto, Ontario, Canada
[e] Heart and Stroke/Richard Lewar Center of Excellence, Toronto, Ontario, Canada

ARTICLE INFO

Article history:
Received 20 January 2011
Received in revised form 7 April 2011
Accepted 4 May 2011
Available online 10 May 2011

Keywords:
Gradient
Vascular endothelial growth factor
Tissue engineering
Collagen
Immobilization

ABSTRACT

A key challenge in tissue engineering is overcoming cell death in the scaffold interior due to the limited diffusion of oxygen and nutrients therein. We here hypothesize that immobilizing a gradient of a growth/survival factor from the periphery to the center of a porous scaffold would guide endothelial cells into the interior of the scaffold, thus overcoming a necrotic core. Proteins were immobilized by one of three methods on porous collagen scaffolds for cardiovascular tissue engineering. The proteins were first activated with 1-ethyl-3-(3-dimethylaminopropyl)carbodiimide/sulfo N-hydroxysuccinimide and then applied to the scaffold by one of three methods to establish the gradient: perfusion (the flow method), use of a source and a sink (the source–sink method) or by injecting 5 μl of the solution at the center of the scaffold (point source method). Due to the high reproducibility and ease of application of the point source method it was further used for VEGF-165 gradient formation, where an ~2 ng ml^{-1} mm^{-1} gradient was formed in a radial direction across a scaffold, 12 mm in diameter and 2.5 mm thick. More endothelial cells were guided by the VEGF-165 gradient deep into the center of the scaffold compared with both uniformly immobilized VEGF-165 (with the same total VEGF concentration) and VEGF-free controls. All scaffolds (including the controls) yielded the same number of cells, but notably the VEGF-165 gradient scaffolds demonstrated a higher cell density in the centre. Thus we concluded that the VEGF-165 gradient promoted the migration, but not proliferation, of cells into the scaffold. These gradient scaffolds provide the foundation for future in vivo tissue engineering studies.

1. Introduction

Myocardial infarction (MI) is a leading cause of death in the USA; nearly 8,000,000 people have suffered from MI and 800,000 new cases occur each year [1]. Due to the inability of heart cells to regenerate and a lack of availability of organs for transplantation this condition is presently incurable [2]. Hence, research into alternative tissue engineering strategies, such as cell injection and engineered heart tissues (EHT), continues to draw attention. An underlying problem of many previously reported EHT is that they mainly rely on diffusion for oxygen and nutrient transfer, which limits their thickness to approximately 100–200 μm [2], far from the physiological thickness of the myocardium (~1 cm). This also results in an uneven cell distribution within the scaffold, with large areas of cell death towards the center. The live cell distribution corresponds well with the oxygen profile within the scaffold, which shows a decreasing oxygen concentration from the periphery of the scaffold towards the center [2].

Although strategies have been proposed to enhance cell survival during the cultivation phase of an EHT, such as supplementing the culture medium with oxygen carriers [3] and using perfusion bioreactors [4,5], cell death still occurs within the scaffolds upon implantation once these external in vitro factors are no longer present. Most of the cell death occurs within 3–7 days post-implantation [6], during which time native blood vessels grow into the construct. To overcome the problem of cell death an ideal strategy would include preforming vascular-like structures within the construct, as has been reported [7–10] and a mechanism to guide infiltration of the host vasculature into the construct upon implantation. Importantly, the pore size in scaffolds can be controlled to accelerate angiogenesis upon implantation [11].

We hypothesized that immobilizing a gradient of a growth/survival factor in the opposite direction to the oxygen gradient would enable cell guidance into the interior of a scaffold for cardiovascular tissue engineering. We used vascular endothelial growth factor

* Corresponding authors. Tel.: +1 416 946 5295; fax: +1 416 978 4317 (M. Radisic), tel.: +1 416 978 1460 (M. Shoichet).
E-mail addresses: molly.shoichet@utoronto.ca (M. Shoichet), m.radisic@utoronto.ca, milica@chem-eng.utoronto.ca (M. Radisic).

1742-7061/$ - see front matter © 2011 Acta Materialia Inc. Published by Elsevier Ltd. All rights reserved.
doi:10.1016/j.actbio.2011.05.002

(VEGF-165) as the growth/survival factor and D4T endothelial cells as a model cell type. Immobilization of biomolecular cues, such as growth factors, onto tissue engineering scaffolds has been investigated in several studies [12,13]. Immobilized growth factors provide localized and prolonged cell stimulation because their rate of internalization is reduced and they have a longer half-life [14,15].

Immobilization of VEGF-165 on biomaterials, a key factor in the process of new blood vessel formation, has been explored in several previous studies. Although a family of VEGF exist from VEGF-A to VEGF-E, an isoform of VEGF-A, VEGF-165, is the most prevalent and well studied [16]. Shen et al. observed increased endothelial cell number and infiltration on collagen scaffolds with uniformly immobilized VEGF-165 [17]. Upon implantation of scaffolds with uniformly immobilized VEGF-165 into right ventricular wall defects in rat hearts enhanced angiogenesis and patch stability were observed compared with VEGF-free controls [18]. We also uniformly immobilized VEGF-165 in combination with angiopoietin-1 onto collagen scaffolds. An increased cell density and proliferation were observed on co-immobilized scaffolds vs. the controls without growth factors in vitro, and increased vessel density was observed in the co-immobilized scaffolds implanted onto chicken chorio-allantoic membrane (CAM) [19]. Koch et al. uniformly immobilized a modified VEGF-165 onto collagen matrices and observed a small but significant angiogenic effect of immobilized VEGF-165 in a CAM assay [20]. Taguchi et al. uniformly co-immobilized VEGF-165 with fibronectin onto poly(acrylic acid) grafted polyethylene films using water soluble carbodiimide chemistry and observed increased cell growth of human umbilical vein endothelial cells [21].

Gradients of growth factors are known to induce chemotactic cell migration. Endothelial cell migration is an essential component in the process of angiogenesis and is mediated by VEGF gradients [22]. Most attempts at investigating VEGF gradients have been carried out in microfluidic devices at the micrometer scale, a powerful approach that enables the chemotactic properties of a particular growth factor/cell type pair to be screened [23,24]. The guidance potential of an immobilized VEGF-165 gradient was recently proven by studying the migration of human microvascular endothelial cells in a three-dimensional (3-D) agarose hydrogel. The constructs with an immobilized gradient of VEGF-165, created using two photon laser-guided chemistry, exhibited a deeper infiltration of endothelial cell filopodia compared with uniform and blank controls [25].

Since porous or fibrous scaffolds are generally translucent or opaque, previous methods to generate gradients, such as laser-guided chemistry [25], cannot be used for the generation of micron to millimeter scale gradients of immobilized growth factors. Thus, alternative approaches are required. Methods to generate growth factor gradients concurrently with the fabrication of porous scaffolds are available. For example, dye-loaded poly(D,L-lactide–co-glycolide) (PLG) microparticles were assembled into multilayered or gradient scaffolds by ethanol treatment, where the concentration of the released molecule can be spatially controlled within the scaffold [26]. Gradients of soluble bone morphogenetic protein 4 and Insulin-like growth factor 1 were created over 30 mm length scales by incorporating protein-loaded silk microspheres into fibrous silk scaffolds [27]. Gradient makers were also utilized to generate gradients of nerve growth factor and neurotrophin-3 during polymerization and fabrication of poly(2-hydroxyethylmethacrylate)/poly(L-lysine) scaffolds [28].

The goals of the study were to: (1) develop a method to immobilize growth factor concentration gradients in a non-transparent preformed porous scaffold; (2) demonstrate cell migration on the scaffold in response to this gradient. To this end we tested three methods to create gradients in the collagen scaffolds and then chose the best one to generate immobilized VEGF-165 gradients using a water-based chemistry. We analyzed the effect of the gradient on endothelial cell distribution in the collagen scaffolds. Ultimately we aim to take advantage of the synergistic effects of cell migration within a VEGF-165 gradient-containing scaffold to promote host tissue integration by guiding host endothelial cells into the scaffold, as a step closer to developing a vascular system within the construct.

2. Materials and methods

2.1. Scaffold preparation

An FDA approved collagen scaffold was used for this project (Ultrafoam collagen sponge, Davol, 1050050). This is a highly porous collagen sponge with pore sizes ranging between 100 and 200 μm [17]. A sterile sheet of the scaffold was cut into the desired shape, a circle or rectangle, with either a circular autoclaved metal cork borer or autoclaved metal scissors, respectively. The diameter of the dry scaffold discs used throughout this project was 12 mm, except for the study to choose an appropriate digestive enzyme for the scaffold (Supplementary Methods), where the diameter was 7 mm. The thickness of the dry scaffold was 2.5 mm. The dimensions of the square scaffolds were 5 × 6 mm.

2.2. Gradient generation methods

To generate gradients of bioactive molecules in porous scaffolds a solution containing the bioactive molecule was applied to the scaffold according to one of the methods described below. For covalent immobilization the biomolecules were first activated with 1-ethyl-3-(3-dimethylaminopropyl)carbodiimide/sulfo-N-hydroxysuccinimide (EDC/S-NHS) and then applied to the collagen scaffold.

2.2.1. The flow method

A circular scaffold was placed tightly between two metal meshes and silicone O-rings and positioned in a polycarbonate bioreactor used in previous cardiac tissue engineering studies [5,29] (Fig. 1A). Tygon tubing (5 mm in diameter, 5 cm long) was attached to the inlet and outlet from the bioreactor and connected to 5 ml syringes via two 3-way valves at each end (Fig. 1A). Two 1 ml syringes (BD, 309628) were connected to the 3-way valves in order to remove any bubbles from the circuit. After mounting the circular scaffold in the bioreactor, the 5 ml syringe at the top end of the bioreactor was filled with phosphate-buffered saline (PBS). The PBS was slowly injected through the circuit into the other syringe in order to wet the scaffold. Once the entire circuit was filled with PBS the 3-way valve at the top end of the bioreactor was closed to the 5 ml syringe and opened to the 1 ml syringe filled with the solution of interest. The solution was slowly (~100 μl in 5 s) injected through the 3-way valve and through the center of the stream and the collagen scaffold. The circuit was then drained through the 5 ml syringe at the bottom of the bioreactor. The scaffold was taken out of the bioreactor and washed twice in 1 ml of PBS to remove the excess solution of interest.

2.2.2. The source–sink method

In this method the scaffold was mounted between two reservoirs as shown in Fig. 1C. The dimensions of the scaffold mount and the scaffold were 5 × 6 mm. The device was engraved on a 5 mm thick polycarbonate sheet (McMaster Carr) using a counter-top milling machine (Roland Modela 3D Plotter MDX-15) equipped with a 1/32 inch tip drill bit (Roland EMF-125-3F-031). Virtual Modela software was used to align the drill bit with the polycarbonate sheet surface. Then Dr. Engrave was used to engrave

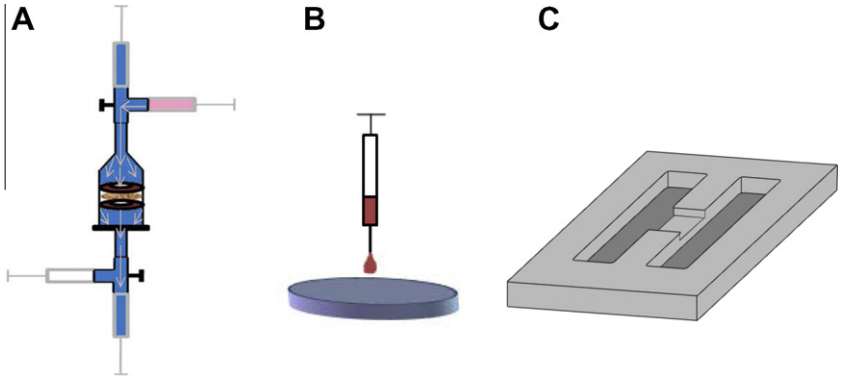

Fig. 1. Overview of the gradient generation methods. (A) The flow method. The scaffold was placed in a bioreactor connected to two syringes at both ends. The scaffold was first perfused with PBS solution (blue). Another syringe with the solution of interest was then used to inject the solution through the center of the scaffold (red arrows). The solution passed through the center of the scaffold and diffused towards the periphery. (B) The point source method. The wet scaffold was placed on a flat surface. The solution of interest was then introduced in the center of the scaffold using a mounted syringe and diffused outwards in a radial direction. (C) The source–sink method. The polycarbonate device was engraved using a counter-top milling machine. The scaffold was mounted at the center of the platform. The source compartment contained the solution of interest and the sink compartment contained the blank PBS solution. The solution of interest diffused from the source compartment to the sink through the scaffold.

the design to a depth of 1.5 mm (scaffold platform) and 2 mm (reservoirs), resulting in the device shown in Fig. 1C.

The scaffold was first immersed in 250 μl of PBS in a 96-well plate for 10 min. The platform on the device was coated with a thin layer of vacuum grease to form a seal. After 10 min the scaffold was dabbed on a Kim wipe to remove excess liquid and transferred to the platform of the device. A glass coverslip was cut into a square piece 3 × 3 cm that would fit on top of the scaffold and act to hold it in place from above. The surface of the coverslip in contact with the scaffold was also coated with vacuum grease in order to prevent leakage of the solutions. The coverslip was then placed on top of the scaffold and a weight of 300–400 g was placed on it to provide pressure from above and seal the scaffold. Subsequently the source and sink reservoirs were filled with 250 μl of the solution of interest and 250 μl of PBS, respectively. The scaffold was treated for 1, 2 or 4 h. The solutions in the two reservoirs were then removed using a 200 μl pipette. The glass coverslip was carefully and slowly lifted off the scaffold and the scaffold was transferred to 500 μl of PBS using tweezers. After immersion for 5 min the scaffold was dabbed on a Kim wipe to remove excess liquid.

2.2.3. Point source method

The scaffold discs were placed in 400 μl of PBS in a 48-well plate for 20 min in order to pre-wet the scaffold. The scaffolds were then placed on autoclaved Kim wipes to remove excess fluid and then transferred to a new 24-well plate. The scaffolds were spread across the plate surface with autoclaved tweezers. Next, a 10 μl glass syringe (Hamilton 7653-01) filled with the solution of interest was mounted on a micromanipulator in an upright position and positioned ~2 inches above the center of the scaffold (Fig. 1B). The syringe was equipped with a 22 gauge needle (Hamilton 7770-02) and was then lowered slowly using the micromanipulator until the needle tip touched the scaffold surface. The solution (5 μl) was then injected into the scaffold. After 1 h the process was repeated twice more. After the third injection the scaffolds were washed eight times in 1 ml of PBS for 5 min per wash.

2.3. Concentration profile characterization

The concentration profiles formed by the gradient generation methods were visualized using 1 mg ml^{-1} bovine serum albumin (BSA) conjugated with a fluorescent dye (Alexa-594) (Invitrogen A13101). After washing the scaffold eight times in 1 ml of PBS it was placed on a glass slide and imaged under a fluorescence microscope at an excitation of 590 nm and emission of 622 nm. The images were viewed in ImageJ (US National Institutes of Health) and the Plot Profile function was used to quantify the fluorescence intensity as a function of the horizontal position on the scaffold. Insets in Fig. 2 show the position of the boxes drawn to characterize the plot profiles.

2.4. Method validation

Further validation of the point source method was carried out by quantifying the fluorescence intensity of Alexa-594-conjugated BSA. In order to quantify the amount of protein in the scaffold the circular scaffold was sectioned into three rings of increasing diameter (a 2 mm diameter disc, a ring with 2 mm inner diameter and 6 mm outer diameter, and a ring with 6 mm inner diameter and 12 mm outer diameter) using two borers of different sizes (2 and 6 mm). Each of the rings were then immersed in 150 μl of 0.276 mg ml^{-1} collagenase type IA (Sigma Aldrich C9891) in a 96-well plate for 1 h for digestion. Several collagen digestion enzymes were tested for their effect on VEGF-165 and collagenase type IA was confirmed to have no effect on VEGF-165 detection (Fig. S1). Following this the plate was read in a fluorescence spectrophotometer (Molecular Device Gemini EM) at 590 nm excitation and 622 nm emission to quantify the amount of Alexa-594-BSA on the scaffold.

For further validation a model protein, horseradish peroxidase (HRP), was covalently immobilized on the scaffold. HRP is a 44 kDa protein that contains free amine and carboxyl groups that can participate in the EDC/S-NHS reaction with the carboxyl groups in the collagen scaffold. To first confirm the compatibility of HRP with EDC/S-NHS chemistry it was immobilized uniformly within collagen scaffolds. For this the scaffolds were activated in 250 μl of 24 mg EDC + 60 mg S-NHS ml^{-1} in PBS (Sigma Aldrich 16142, Pierce 24510) for 20 min and transferred to 250 μl of 0.01, 0.1 or 1 mg ml^{-1} HRP in PBS at room temperature for 1 h. Following the reaction the scaffolds were washed eight times in 1 ml of PBS for 5 min per wash. A gradient of HRP was created in new scaffolds using the point source method described above using a solution of 0.01 mg ml^{-1} HRP and 24 mg EDC + 60 mg S-NHS ml^{-1} in PBS for scaffold activation. The scaffold was sectioned into rings as described above and digested with collagenase. To quantify the amount of HRP present in the digested solution 100 μl of 2,2′-azino-bis(3-ethylbenzothiazoline-6-sulfonic acid) (ABTS) (Sigma Aldrich A3219) was added to 100 μl of scaffold solution. ABTS is

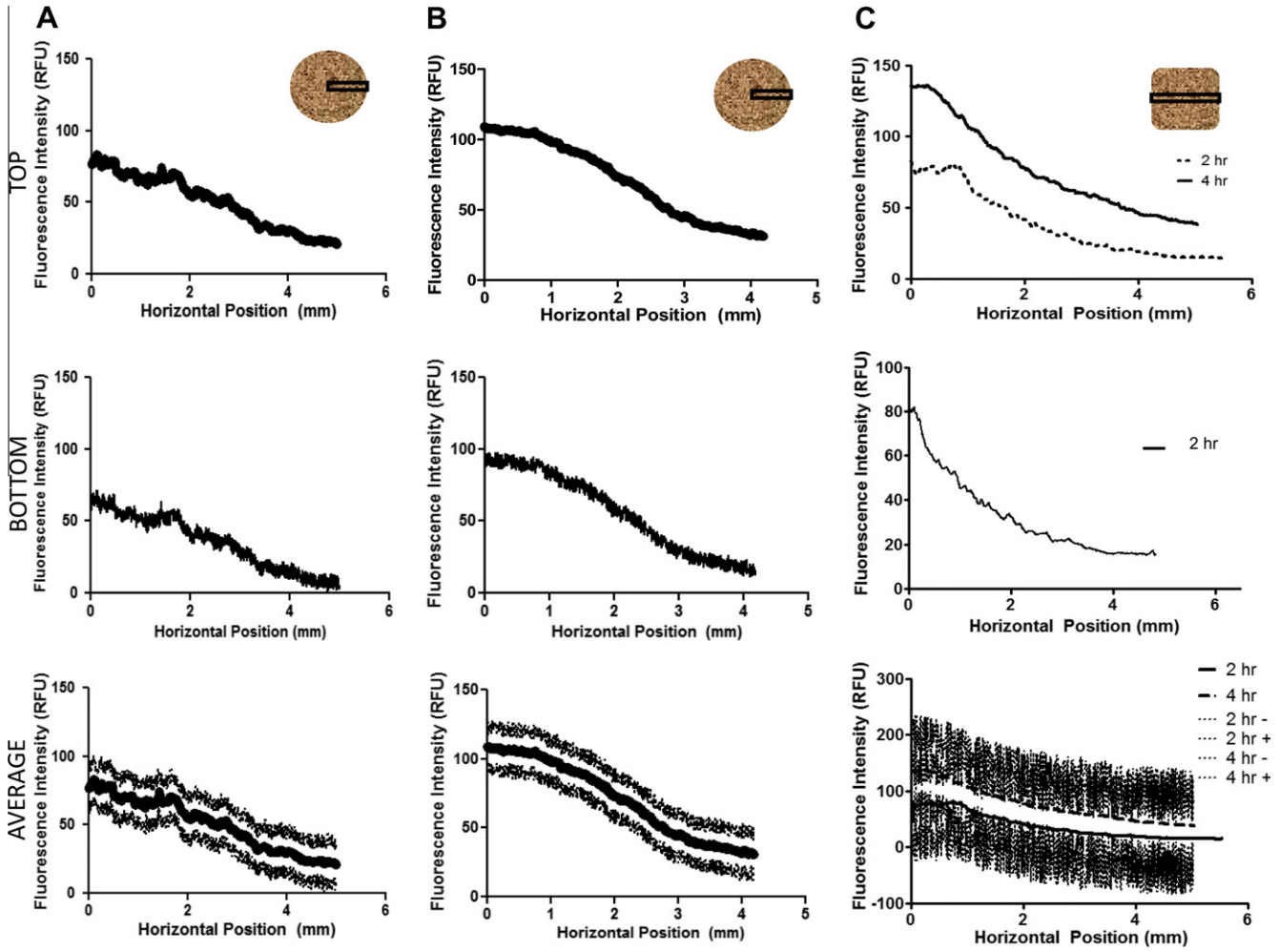

Fig. 2. Fluorescence intensity profiles of Alexa-594-BSA for the three gradient generation methods. (A) The flow method. (B) The point source method. (C) The source–sink method. (Top) A representative profile as it appears looking from the top of the scaffold, as shown in the insets. (Bottom) A representative profile as it appears looking from the bottom of the scaffold. (Average) Average (solid line) and standard deviation (the dashed lines above and below the curve) for the fluorescence intensity profiles collected from the tops of $n = 3$ different scaffolds. The zero point on the x-axis corresponds to the center of the scaffold in (A) and (B) and the source edge of the scaffold in (C). As expected, both (A) and (B) show the highest concentration at the center of the scaffold, the point of injection of the dye, which then drops off moving towards the periphery. Similarly, (C) shows the highest concentration at the source edge of the scaffold, which drops off moving towards the sink side.

a substrate for HRP that undergoes a colorimetric reaction within a time span of ~5 min. The color change was monitored on a plate reader (Apollo LB911) at 405 nm. The amount of HRP was calculated based on standard curves of known amounts of HRP and expressed as a concentration by calculating the volume of each circular section.

2.5. VEGF immobilization and quantification

The point source method was used to create a VEGF-165 gradient in a collagen scaffold via the EDC/S-NHS chemistry as described above using a syringe filled with 1 μg ml^{-1} murine VEGF-165 (Peprotech, 900-K99) and 24 mg EDC + 60 mg S-NHS ml^{-1} in PBS. The solution was injected into the center of the scaffold in 5 μl volumes either once or three times, leaving 1 h for the reaction following each injection. The solution was prepared fresh before each injection. The scaffolds were then washed eight times in 1 ml of PBS for 5 min for each wash. Scaffolds with uniformly immobilized VEGF-165 and no VEGF-165 were used as the controls. For uniform immobilization the scaffolds were first activated in 250 μl of 12 mg EDC + 30 mg S-NHS ml^{-1} in PBS for 20 min in a 24-well plate. They were then transferred to a fresh well containing 250 μl of a 100 ng ml^{-1} solution of VEGF-165 for 1 h. Blank scaffolds containing no VEGF-165 were prepared in the same way as the gradient scaffolds described above, with the only change being the absence of VEGF-165 in the solution of interest. Both the blank and the uniform scaffolds were subjected to eight washes in 1 ml of PBS for 5 min per wash.

After processing and digesting the cut scaffold sections as described above the solutions were analyzed using a murine sandwich ELISA kit for VEGF-165 (Peprotech 900-K99). For this the manufacturer's protocol was followed, the only modification being that instead of using the manufacturer supplied VEGF-165 as the standard the VEGF-165 that was used for immobilization in the experiments was used. The results are expressed as the VEGF-165 concentration detected in the given scaffold section digestate by dividing the total amount of VEGF-165 detected in each section by the calculated section volume.

2.6. Cell studies

2.6.1. Cell culture

D4T endothelial cells (EC), an embryoid body-derived mouse EC line, was used according to our previously published protocol

[17,30]. The cells were propagated in culture medium (D4T medium) consisting of Iscove's modified Dulbecco's medium (IMDM) (Gibco 12440-053) with 5% fetal bovine serum (FBS) (Gibco 16000-044), 100 units ml^{-1} penicillin, and 100 μg ml^{-1} streptomycin (Gibco/Invitrogen 15140122) [31]. The cells used in this study were between passages 10 and 20.

2.6.2. Cell migration study

Following immobilization of the growth factor on the scaffold the scaffolds were placed in 500 μl of D4T culture medium in a 37 °C/5% CO_2 incubator for 30 min. They were then placed at the bottom of a 48-well tissue culture plate (BD Scientific 353230) and the cell suspension (5000 cells per 500 μl culture medium) was added on top of the scaffolds. The plate was centrifuged at 140 r.c.f. for 5 min in a plate centrifuge to force the cells uniformly into the scaffold pores. There were three experimental groups: (i) scaffolds with a VEGF-165 gradient; (ii) scaffolds with uniformly immobilized VEGF-165; (iii) scaffolds with no VEGF-165. After the centrifugation step the remaining culture medium was aspirated off and the scaffolds were placed in a 37 °C/5% CO_2 incubator for 40 min for the cells to attach to the scaffold. Then 1 ml of culture medium was added to each well containing the scaffold and the plate was returned to the incubator. After 3 days culture the scaffolds were removed from the incubator. The culture medium was aspirated and the scaffolds were stained using Live/Dead markers by incubating the scaffolds in 400 μl of staining solution (1.5 μl of carboxyfluorescein diacetate and 75 μl of propidium iodide in 1 ml of PBS) for 40 min, as published previously [30]. The scaffolds were then imaged under a fluorescence microscope with the blue filter in order to visualize live cells. To study the cell distribution on the scaffold, images were taken at 4× along the two diameter axes on the scaffold. The surface on which the cells were spun down, i.e. the top surface, was imaged for each scaffold. Serial images were taken along the axes and the cell count in each image was determined using the ImageJ cell counter function. To maintain consistency only cells in the top layer (and not the bleed through) were counted in each image.

To determine the cross-sectional spatial distribution of cells on day 3 the cell-seeded scaffolds ($n = 4$ per group) were fixed in 10% formalin for 1 h at room temperature. The scaffolds were then cut in half through the centerline such that the cross-section at the center of the sample was revealed. The cross-section of each sample was placed face down in a cryomold with OCT medium and snap frozen with liquid nitrogen as described [17]. The snap frozen samples were cryosectioned at −22 °C at a thickness of 10 μm. The sections were stained with 4′,6-diamidino-2-phenylindole (DAPI) and imaged using fluorescence microscopy.

2.7. Statistical analysis

Statistical significance in comparisons between different groups was determined by one-way ANOVA in conjunction with Tukey's post hoc test using GraphPad Prism. $P < 0.05$ was considered significant.

3. Results and discussion

Representative radial fluorescence intensity profiles of Alexa-594-BSA for all three methods are shown in Fig. 2. Both the flow (Fig. 2A) and point source (Fig. 2B) methods resulted in the expected radial profiles, with the scaffold showing the highest fluorescence intensity as the solution of interest penetrated the scaffold in the center and diffused towards the periphery. Consequently, the intensity dropped from the center towards the periphery. The concentration profile of the source–sink (Fig. 2C) method was different from the other two methods, as the solution of interest penetrated the scaffold on one side and diffused towards the other. Hence the intensity profile was highest on the side closest to the reservoir containing the solution of interest and lowest on the blank reservoir side. The resulting profile was dependent on the time period allowed for diffusion, with higher fluorescence intensity at 4 h vs. 2 h. There were no appreciable differences in the fluorescence intensity profiles collected from the top versus the bottom of the scaffolds for the flow and point source methods (Fig. 2A and B). However, there were noticeable differences in the top vs. bottom lines collected for the source–sink method (Fig. 2C).

In comparison with the source–sink method the point source and flow methods offered superior reproducibility, as shown by the larger spread of the data points around the average value for the source–sink method (Fig. 2C). In addition, these two methods generated a radial gradient starting in the center, in contrast to the linear gradient generated by the source–sink method. The radial gradient meets our design criteria of promoting cell migration towards the scaffold center. Of these two methods the point source method provided a smoother profile and was technically simpler than the flow method. Importantly, the point source method uses significantly smaller amounts of reagents because all of the starting solution of interest is injected into the scaffold. Hence, only the point source method was evaluated further.

The gradients of three different proteins processed by the point source method were compared by quantifying the concentration in three concentric circular rings of the collagen scaffold after digestion by collagenase: Alexa-594-BSA, HRP and VEGF-165 (Fig. 3). The intensity profile was normalized to the volume of each of the collagen scaffold rings. HRP has a similar molar mass to VEGF-165 and was used previously as a model protein for covalent immobilization of linear gradients in 12 mm thick porous silk scaffolds [32]. As expected, it was found that the HRP concentration immobilized uniformly into collagen scaffolds was dependent on the HRP concentration in the immobilization solution (Fig. S2). Since 0.01 mg ml^{-1} HRP in the immobilization solution showed the greatest difference between the immobilized and physically adsorbed HRP, it was used for further validation studies. As expected, the center regions of the scaffold contained the maximum amount of protein, since the protein solution was introduced there. The amount of protein decreased from the center towards the periphery. Interestingly, three serial injections of VEGF-165 solutions led to a 3.8 ± 0.4 times higher amount of VEGF-165 immobilized (0.27 ± 0.03 ng) compared with one injection (0.07 ± 0.01 ng). In addition, the gradient was steeper with three serial injections (2.35 ng ml^{-1} mm^{-1}) compared with a single injection (0.64 ng ml^{-1} mm^{-1}) (Fig. 3C). Interestingly, although HRP was applied at 10 μg ml^{-1} and VEGF-165 at 1 μg ml^{-1}, no appreciable differences in the center concentrations were observed after immobilization (Fig. 3B and C). It is likely the reaction was limited by the amount of cross-linker or the period of time carboxyl groups remained activated.

The bioactivity of VEGF-165 has been previously reported to be either unaffected or enhanced due to covalent immobilization. Aizawa et al. measured the proliferation of EC in the presence of either immobilized or soluble forms of VEGF-165. It was found that for approximately the same amounts of VEGF-165 the cells showed no difference in proliferation between the immobilized and soluble groups [25]. Chiu and Radisic found that endothelial cells proliferated significantly more on collagen scaffolds with immobilized VEGF-165 and angiopoietin-1 than on scaffolds supplemented with soluble forms of the same growth factors [19]. We took advantage of the extensive studies done to differentiate between physical adsorption and covalent modification using identical synthetic techniques [19] and focused simply on scaffolds containing immobilized VEGF-165 and the resulting cell guidance.

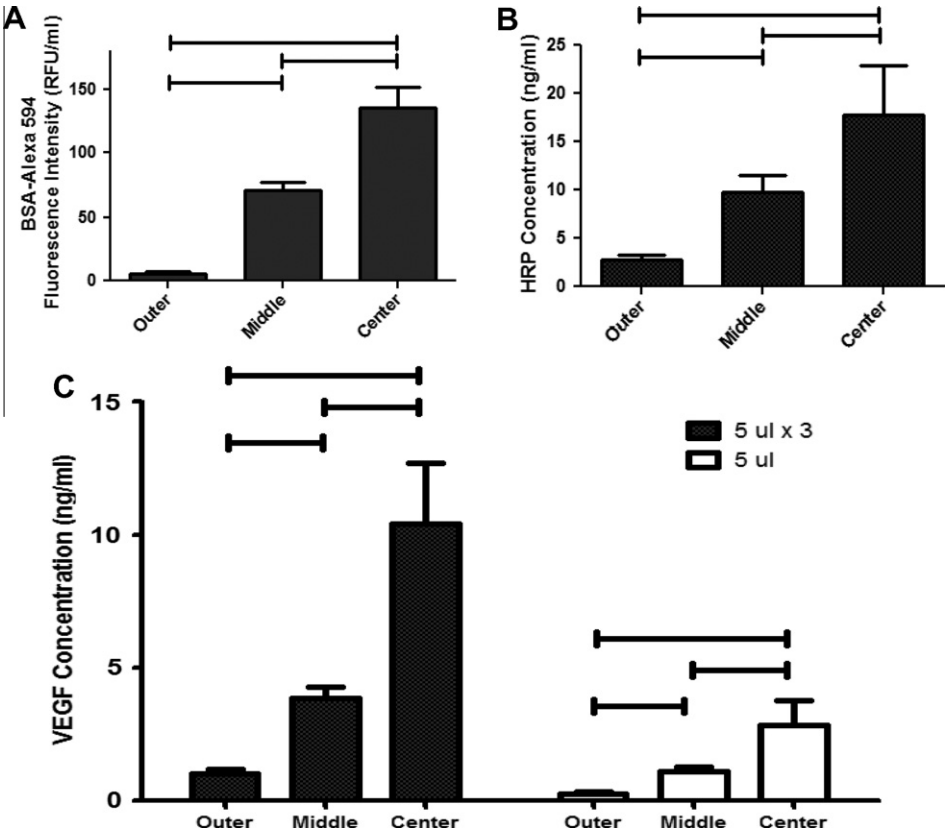

Fig. 3. Protein quantification for the point source method. Scaffolds were either injected with Alexa-594-labeled BSA or HRP or VEGF for covalent immobilization using the point source method. The scaffolds were then sectioned into three concentric rings and digested with collagenase. The protein content in each ring was measured and normalized to the calculated volume. (A) Alexa 594-BSA; (B) HRP; (C) VEGF. Error bars indicate standard deviations. Horizontal lines above the bars indicate a statistically significant difference ($P < 0.05$, $n = 4–6$).

Having created well-defined concentration gradient scaffolds we next examined the cell distribution on the scaffolds with a VEGF-165 gradient vs. a homogeneous concentration of VEGF-165 vs. no VEGF-165 (controls). Centrifuging the cells into the scaffold did not affect cell viability, since the great majority of cells were viable immediately after seeding (Fig. S3). In addition, the cell distribution at the top scaffold surface was uniform immediately after seeding (Fig. S4). As shown in Fig. 4 for the top scaffold surface, the scaffolds with the gradient of VEGF-165 resulted in a distribution of cells at the end of 3 days cultivation that mirrored the VEGF-165 gradient, with a higher cell concentration in the center and a lower one at the periphery. The scaffolds with uniform VEGF-165 had a distribution that also mirrored the concentration of VEGF-165, i.e. a relatively uniform cell distribution along the radius. Similarly, the scaffolds without immobilized VEGF-165 had a relatively uniform distribution of cells, but showed a trend towards a lower total cell number compared with the scaffolds with uniformly immobilized VEGF-165. Importantly, the total amount of immobilized VEGF-165 was comparable (and not significantly different) in the gradient scaffold (0.27 ± 0.03 ng) and uniformly immobilized scaffold (0.38 ± 0.09 ng). In addition, DAPI stained cross-sections of the scaffolds ($n = 4$ per group, Fig. 5) confirmed a greater presence of cells in the central cross-section of the gradient scaffolds compared with the no VEGF controls and also scaffolds with uniformly immobilized VEGF.

The concentration of immobilized VEGF-165 used in this study was between 3 and 10 ng ml^{-1}. Previous reports of immobilized VEGF-165 have observed the cell response to a broad range of concentrations. There are reports of high concentrations of VEGF-165: Aizawa et al. examined concentrations of the order of 400–2000 ng ml^{-1} [25]; Chiu and Radisic used concentrations of approximately 750 ng ml^{-1} [19]; Shen et al. reported concentrations of 40 and 110 ng ml^{-1} on collagen scaffolds [17]. There are also reports of lower concentrations of VEGF-165: Chung et al. used concentration gradients ranging between 0 and 20 ng ml^{-1} in a microfluidic channel [24]; Shamloo et al. used concentrations ranging between 18 and 32 ng ml^{-1}, with the average concentration being 25 ng ml^{-1}, in soluble form [23]. Hence, there is a wide concentration range over which EC in general, and D4T EC in particular, respond to VEGF-165. Interestingly, the results of the current study confirm that D4T EC are able to respond to VEGF-165 cues in the range 3–10 ng ml^{-1}.

The cell distribution profile for the gradient scaffolds shows a Gaussian-like profile where more cells are present in the center region of the scaffold, thereby mimicking the VEGF-165 gradient, which is also highest in the center. The correlation of VEGF-165 gradient with cell distribution suggests that the D4T cells are either guided up the VEGF-165 concentration gradient on the collagen scaffolds or that they proliferate more in the center, at the higher immobilized VEGF-165 concentration. The scaffolds with uniformly immobilized VEGF-165 did not exhibit any particular spatial preference for the cells. This was expected, since cells detect similar amounts of VEGF-165 at all points on the scaffold. Similarly, the blank scaffolds did not show any statistically significant trend in cell distribution.

The distribution of cells after 3 days on the scaffolds raises an important question: are the cells proliferating/surviving selectively or migrating in response to the VEGF-165 gradient in the scaffold? Chiu and Radisic reported that collagen scaffolds uniformly immobilized with VEGF-165 showed a significantly higher number of

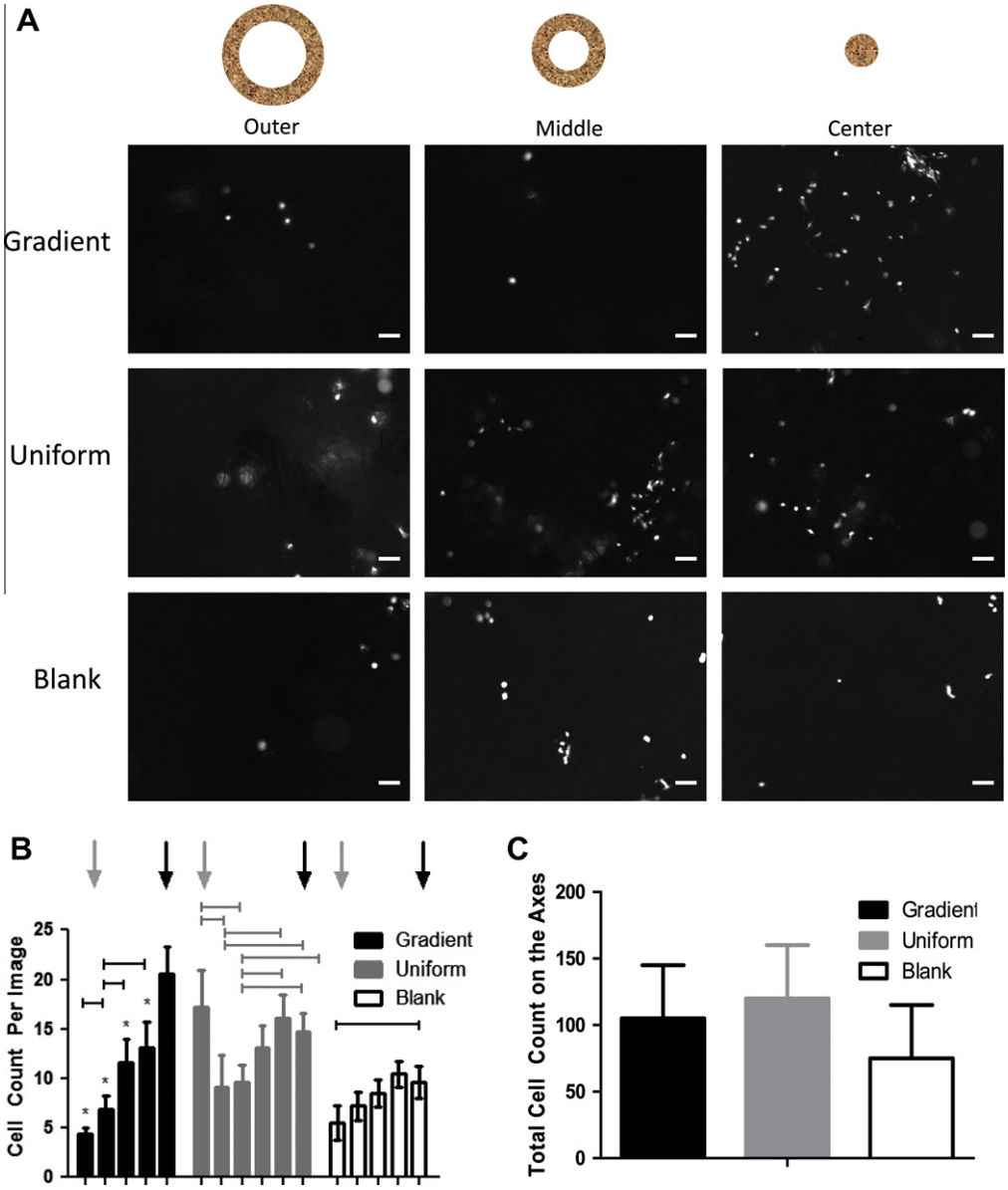

Fig. 4. Scaffolds with VEGF gradients lead to a more centralized cell distribution. (A) The scaffolds prepared by the point source method were seeded with 5000 cells and cultured for 3 days. At the end of the culture period the scaffolds were stained with a live cell marker, CFDA. Serial images were acquired on the two axes of the circular scaffold. (B) The cell density of each image was counted using ImageJ. The plot shows the cell distribution on the scaffolds. The *x*-axis spans the radius of the scaffold for each group. Black and white arrows indicate the scaffold center and periphery, respectively. (C) The number of cells along the diameter of the scaffold was calculated by adding the number of cells in each image along the two axes of the scaffold. Error bars indicate standard errors ($n = 4–6$). The stars indicate a statistically significant difference from the highest (center) value. The lines indicate statistically significant differences between groups ($P < 0.05$). Scale bar 500 μm.

cells, suggesting a higher proliferation and survival rate on these scaffolds. In order to determine the exact mechanism of cell behavior the total number of cells per scaffold was counted and found not to be significantly different, as shown in Fig. 4C. This indicates that the cells did not proliferate in response to the immobilized VEGF-165, but instead migrated along the immobilized VEGF-165 gradient of $\sim$2 ng ml^{-1} mm^{-1}. This suggests that the immobilization of VEGF-165, either in a uniform or gradient pattern, does not lead to a greater survival or proliferation of EC over this 3 day time period. This is in contrast to the results reported by Chiu and Radisic [19]. This discrepancy can be explained by two major factors. First, the immobilized concentration in the current system is about two orders of magnitude lower than that in the Chiu study (3–10 vs. 750 ng ml^{-1}). It is possible that lower VEGF-165 levels are able to promote cell migration but not proliferation. Second, the cell density used in this study is lower than that used by Chiu (5000 vs 50,000 cells per scaffold). Since one of the factors that govern cell–cell interaction is cell density, this reduction in cell number is expected to affect the cell response.

We have here described methods that enable us to generate gradients of covalently immobilized growth factors in porous scaffolds. In the envisioned cardiac tissue engineering scenario we plan to generate a gradient of a cardiac survival factor. For example, a gradient of covalently immobilized angiopoietin 1, which acts as a survival factor for cardiomyocytes [33], could be incorporated in a porous scaffold. A high concentration of angiopoietin 1 in the center of the scaffold would enable cardiomyocytes to survive during the tissue engineering process and upon implantation. In addition, a gradient of angiopoietin 1 would promote the ingrowth of blood vessels into the scaffold.

In general, three different cardiac tissue engineering approaches can be identified: (1) the seeding of cells onto preformed porous or

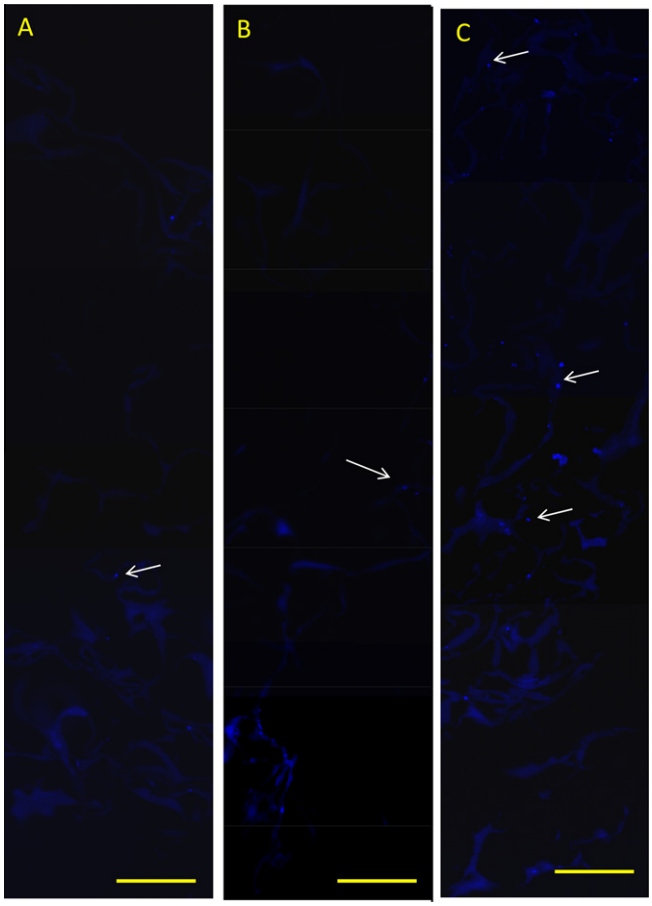

Fig. 5. Cross-sectional cell distribution at the central axis of the scaffolds. (A) Blank (no VEGF control); (B) uniform immobilization of VEGF; (C) gradient immobilization of VEGF. DAPI staining of cell nuclei appears as bright blue dots. White arrows point to representative cell nuclei. Scale bar 100 μm.

fibrous scaffolds followed by bioreactor cultivation; (2) cultivation of cells encapsulated in hydrogels; (3) a matrix-free approach that relies on cardiomyocyte self-assembly or stacking of confluent cell sheets. In addition, encapsulation of cells in hydrogels immediately prior to myocardial injection has also been performed [34–37], however, this approach does not result in contractile cardiac patches in vitro.

Biodegradable scaffolds are designed to provide a flexible structural template for cell attachment and tissue organization. Scaffolds with a gradient of immobilized growth factor such as one described here could thus find utility in the cell–scaffold–bioreactor approach, which aims at cultivating cardiac tissues under biomimetic conditions [38]. Previously, cardiac grafts expressing the structural and physiological features characteristic of native cardiac muscle have been engineered using fetal or neonatal rat cardiac myocyte-enriched cell populations with both natural polymers (collagen [4] and alginate [7]) and synthetic polymers (polyglycolic acid [39–44]). The primary advantage of utilizing scaffolds is that they can be tailored to any size or shape and their mechanical properties can be precisely controlled. Suggested disadvantages of porous and fibrous scaffolds include limited development of contractile force due to the inherent stiffness of the scaffold, incomplete biodegradation and poor cell alignment and morphology. Hydrogels, on the other hand, exhibit no mechanical or spatial restrictions [45], thus they were utilized in pioneering cardiac tissue engineering studies that resulted in highly differentiated contractile cardiac muscle [46,47].

Contractile cardiac grafts can also be engineered without the use of matrix materials by stacking monolayered cell sheets released from a temperature-responsive polymer (poly-N-isopropylacrylamide) that is cell non-adhesive below 32°C [10,48–50]. These cell sheets were then overlaid to form grafts; extracellular matrix produced by the cells acts as an adhesive holding the cell sheets together. The cell sheet technology allows manipulation to form various graft shapes. A current limitation, however, includes graft thickness in vitro, which is limited to 3–4 cell layers. Other matrix-free self-organization approaches include spontaneous wrapping of confluent monolayers around a poly(glycolic acid) string [51].

The creation of growth factor gradients in collagen scaffolds as described here represents an important advance, since photochemical and lithographic techniques would not work in opaque porous scaffolds. The point source method, albeit simple, was effective in creating a gradient of immobilized VEGF-165 in the scaffold and could be extended to many other porous scaffold types, since it utilizes water soluble EDC chemistry at physiological pH. The method enables gradient generation in preformed scaffolds without the need to polymerize/fabricate the scaffold concurrently with gradient generation. The collagen scaffolds used here have already been demonstrated to be cytocompatible in vitro and biocompatible in vivo, thus the ability to guide cells deeper into the scaffold interior may overcome the formation of a necrotic core normally observed during the tissue engineering process and upon implantation. Importantly, gradient creation was achieved on millimeterscale scaffolds, which is larger than most microscale systems and thus closer to the clinical requirements [23,24].

4. Conclusions

We have reported three methods of generating protein gradients on collagen scaffolds, with the point source method being the most facile and reproducible of the three tested. The VEGF-165 gradient ($\sim$2 ng ml^{-1} mm^{-1}) immobilized in a radial direction in a 12 mm diameter collagen scaffold guided EC deep into the center of the scaffold, compared with the uniformly immobilized VEGF-165 and the VEGF-free controls. The migration of cells deep into the scaffold rather than proliferation in the scaffold interior was substantiated by the similar numbers of cells on the different scaffolds. Interestingly, these effects were observed even with very low concentrations of immobilized VEGF-165, indicating that high concentrations are not necessarily required to observe cell guidance. The developed gradient scaffolds may be used to guide cells into the scaffold interior during the tissue engineering process and upon implantation.

Acknowledgements

This work was funded by a grant from Ontario Centers of Excellence to M.S.S. and M.R. (BM50831), NSERC Discovery Grants to M.R. (RGPIN 326982-10) and M.S.S. (RGPIN 203310-09), NSERC Strategic Grant to M.R. (STPGP 381002-09), and Discovery Accelerator Supplement (RGPAS 396125-10) and Heart and Stroke/Ontario Graduate Scholarship in Science and Technology to D.O.

Appendix A. Figures with essential colour discrimination

Certain figures in this article, particularly Figures 1, 2, 4, and 5, are difficult to interpret in black and white. The full colour images can be found in the on-line version, at doi:10.1016/j.actbio.2011.05.002.

Appendix B. Supplementary data

Supplementary data associated with this article can be found, in the online version, at doi:10.1016/j.actbio.2011.05.002.

References

[1] Association AH. Heart Disease and Stroke Statistics – 2004 Update. Dallas, TX: American Heart Association, 2004.
[2] Radisic M, Malda J, Epping E, Geng W, Langer R, Vunjak-Novakovic G. Oxygen gradients correlate with cell density and cell viability in engineered cardiac tissue. Biotechnol Bioeng 2006;93:332–43.
[3] Radisic M, Park H, Chen F, Salazar-Lazzaro JE, Wang Y, Dennis R, et al. Biomimetic approach to cardiac tissue engineering: oxygen carriers and channeled scaffolds. Tissue Eng 2006;12:2077–91.
[4] Brown MA, Iyer RK, Radisic M. Pulsatile perfusion bioreactor for cardiac tissue engineering. Biotechnol Prog 2008;24:907–20.
[5] Radisic M, Yang L, Boublik J, Cohen RJ, Langer R, Freed LE, et al. Medium perfusion enables engineering of compact and contractile cardiac tissue. Am J Physiol Heart Circ Physiol 2004;286:H507–516.
[6] Jiang F, Zhang G, Hashimoto I, Kumar BS, Bortolotto S, Morrison WA, et al. Neovascularization in an arterio-venous loop-containing tissue engineering chamber: role of NADPH oxidase. J Cell Mol Med 2008;12:2062–72.
[7] Dvir T, Kedem A, Ruvinov E, Levy O, Freeman I, Landa N, et al. Prevascularization of cardiac patch on the omentum improves its therapeutic outcome. Proc Natl Acad Sci USA 2009;106:14990–5.
[8] Stevens KR, Kreutziger KL, Dupras SK, Korte FS, Regnier M, Muskheli V, et al. Physiological function and transplantation of scaffold-free and vascularized human cardiac muscle tissue. Proc Natl Acad Sci USA 2009;106:16568–73.
[9] Levenberg S, Rouwkema J, Macdonald M, Garfein ES, Kohane DS, Darland DC, et al. Engineering vascularized skeletal muscle tissue. Nat Biotechnol 2005;23:879–84.
[10] Asakawa N, Shimizu T, Tsuda Y, Sekiya S, Sasagawa T, Yamato M, et al. Prevascularization of in vitro three-dimensional tissues created by cell sheet engineering. Biomaterials 2010;31:3903–9.
[11] Madden LR, Mortisen DJ, Sussman EM, Dupras SK, Fugate JA, Cuy JL, et al. Proangiogenic scaffolds as functional templates for cardiac tissue engineering. Proc Natl Acad Sci USA 2010;107:15211–6.
[12] Rahman N, Purpura KA, Wylie RG, Zandstra PW, Shoichet MS. The use of vascular endothelial growth factor functionalized agarose to guide pluripotent stem cell aggregates toward blood progenitor cells. Biomaterials 2010;31:8262–70.
[13] Yu LM, Miller FD, Shoichet MS. The use of immobilized neurotrophins to support neuron survival and guide nerve fiber growth in compartmentalized chambers. Biomaterials 2010;31:6987–99.
[14] Kuhl PR, Griffith-Cima LG. Tethered epidermal growth factor as a paradigm for growth factor-induced stimulation from the solid phase. Nat Med 1996;2:1022–7.
[15] Fan VH, Tamama K, Au A, Littrell R, Richardson LB, Wright JW, et al. Tethered epidermal growth factor provides a survival advantage to mesenchymal stem cells. Stem cells 2007;25:1241–51.
[16] Boontheekul T, Mooney DJ. Protein-based signaling systems in tissue engineering. Curr Opin Biotechnol 2003;14:559–65.
[17] Shen YH, Shoichet MS, Radisic M. Vascular endothelial growth factor immobilized in collagen scaffold promotes penetration and proliferation of endothelial cells. Acta Biomater 2008;4:477–89.
[18] Miyagi Y, Chiu LL, Cimini M, Weisel RD, Radisic M, Li RK. Biodegradable collagen patch with covalently immobilized VEGF for myocardial repair. Biomaterials 2010;32:1280–90.
[19] Chiu LL, Radisic M. Scaffolds with covalently immobilized VEGF and angiopoietin-1 for vascularization of engineered tissues. Biomaterials 2010;31:226–41.
[20] Koch S, Yao C, Grieb G, Prevel P, Noah EM, Steffens GC. Enhancing angiogenesis in collagen matrices by covalent incorporation of VEGF. J Mater Sci Mater Med 2006;17:735–41.
[21] Taguchi T, Kishida A, Akashi M, Maruyama I. Immobilization of human vascular endothelial growth factor (VEGF165) onto biomaterials: an evaluation of the biological activity of immobilized VEGF165. J Bioactive Compatible Polym 2000;15:309–20.
[22] Helm CL, Fleury ME, Zisch AH, Boschetti F, Swartz MA. Synergy between interstitial flow and VEGF directs capillary morphogenesis in vitro through a gradient amplification mechanism. Proc Natl Acad Sci USA 2005;102:15779–84.
[23] Shamloo A, Ma N, Poo MM, Sohn LL, Heilshorn SC. Endothelial cell polarization and chemotaxis in a microfluidic device. Lab Chip 2008;8:1292–9.
[24] Chung S, Sudo R, Mack PJ, Wan CR, Vickerman V, Kamm RD. Cell migration into scaffolds under co-culture conditions in a microfluidic platform. Lab Chip 2009;9:269–75.
[25] Aizawa Y, Wylie R, Shoichet M. Endothelial cell guidance in 3D patterned scaffolds. Adv Mater 2010;228:4831–5.
[26] Singh M, Morris CP, Ellis RJ, Detamore MS, Berkland C. Microsphere-based seamless scaffolds containing macroscopic gradients of encapsulated factors for tissue engineering. Tissue Eng C Methods 2008;14:299–309.
[27] Wang X, Wenk E, Zhang X, Meinel L, Vunjak-Novakovic G, Kaplan DL. Growth factor gradients via microsphere delivery in biopolymer scaffolds for osteochondral tissue engineering. J Control Release 2009;134:81–90.
[28] Moore K, MacSween M, Shoichet M. Immobilized concentration gradients of neurotrophic factors guide neurite outgrowth of primary neurons in macroporous scaffolds. Tissue Eng 2006;12:267–78.
[29] Radisic M, Euloth M, Yang L, Langer R, Freed LE, Vunjak-Novakovic G. High-density seeding of myocyte cells for cardiac tissue engineering. Biotechnol Bioeng 2003;82:403–14.
[30] Iyer RK, Chiu LL, Radisic M. Microfabricated poly(ethylene glycol) templates enable rapid screening of triculture conditions for cardiac tissue engineering. J Biomed Mater Res A 2009;89:616–31.
[31] Choi K, Kennedy M, Kazarov A, Papadimitriou JC, Keller G. A common precursor for hematopoietic and endothelial cells. Development 1998;125:725–32.
[32] Vepari CP, Kaplan DL. Covalently immobilized enzyme gradients within three-dimensional porous scaffolds. Biotechnol Bioeng 2006;93:1130–7.
[33] Dallabrida SM, Ismail N, Oberle JR, Himes BE, Rupnick MA. Angiopoietin-1 promotes cardiac and skeletal myocyte survival through integrins. Circ Res 2005;96:e8–24.
[34] Fink C, Ergun S, Kralisch D, Remmers U, Weil J, Eschenhagen T. Chronic stretch of engineered heart tissue induces hypertrophy and functional improvement. FASEB J 2000;14:669–79.
[35] Zimmermann WH, Fink C, Kralish D, Remmers U, Weil J, Eschenhagen T. Three-dimensional engineered heart tissue from neonatal rat cardiac myocytes. Biotechnol Bioeng 2000;68:106–14.
[36] Eschenhagen T, Fink C, Remmers U, Scholz H, Wattchow J, Woil J, et al. Three-dimensional reconstitution of embryonic cardiomyocytes in a collagen matrix: a new heart model system. FASEB J 1997;11:683–94.
[37] Zimmermann WH, Schneiderbanger K, Schubert P, Didie M, Munzel F, Heubach JF, et al. Tissue engineering of a differentiated cardiac muscle construct. Circ Res 2002;90:223–30.
[38] Radisic M, Park H, Gerecht S, Cannizzaro C, Langer R, Vunjak-Novakovic G. Biomimetic approach to cardiac tissue engineering. Philos Trans R Soc Lond B Biol Sci 2007;362:1357–68.
[39] Bursac N, Papadaki M, Cohen RJ, Schoen FJ, Eisenberg SR, Carrier R, et al. Cardiac muscle tissue engineering: toward an in vitro model for electrophysiological studies. Am J Physiol Heart Circ Physiol 1999;277: H433–44.
[40] Carrier RL, Papadaki M, Rupnick M, Schoen FJ, Bursac N, Langer R, et al. Cardiac tissue engineering: cell seeding, cultivation parameters and tissue construct characterization. Biotechnol Bioeng 1999;64:580–9.
[41] Carrier RL, Rupnick M, Langer R, Schoen FJ, Freed LE, Vunjak-Novakovic G. Effects of oxygen on engineered cardiac muscle. Biotechnol Bioeng 2002;78:617–25.
[42] Carrier RL, Rupnick M, Langer R, Schoen FJ, Freed LE, Vunjak-Novakovic G. Perfusion improves tissue architecture of engineered cardiac muscle. Tissue Eng 2002;8:175–88.
[43] Papadaki M, Bursac N, Langer R, Merok J, Vunjak-Novakovic G, Freed LE. Tissue engineering of functional cardiac muscle: molecular, structural and electrophysiological studies. Am J Physiol Heart Circ Physiol 2001;280: H168–78.
[44] Engelmayr Jr GC, Cheng M, Bettinger CJ, Borenstein JT, Langer R, Freed LE. Accordion-like honeycombs for tissue engineering of cardiac anisotropy. Nat Mater 2008;7:1003–10.
[45] Radisic M, Park H, Shing H, Consi T, Schoen FJ, Langer R, et al. Functional assembly of engineered myocardium by electrical stimulation of cardiac myocytes cultured on scaffolds. Proc Natl Acad Sci USA 2004;101:18129–34.
[46] Zimmermann WH, Didie M, Wasmeier GH, Nixdorff U, Hess A, Melnychenko I, et al. Cardiac grafting of engineered heart tissue in syngenic rats. Circulation 2002;106:I151–7.
[47] Zimmermann WH, Melnychenko I, Wasmeier G, Didie M, Naito H, Nixdorff U, et al. Engineered heart tissue grafts improve systolic and diastolic function in infarcted rat hearts. Nat Med 2006;12:452–8.
[48] Shimizu T, Yamato M, Isoi Y, Akutsu T, Setomaru T, Abe K, et al. Fabrication of pulsatile cardiac tissue grafts using a novel 3-dimensional cell sheet manipulation technique and temperature-responsive cell culture surfaces. Circ Res 2002;90:e40–8.
[49] Shimizu T, Sekine H, Isoi Y, Yamato M, Kikuchi A, Okano T. Long-term survival and growth of pulsatile myocardial tissue grafts engineered by the layering of cardiomyocyte sheets. Tissue Eng 2006;12(3):499–507.
[50] Shimizu T, Sekine H, Yang J, Isoi Y, Yamato M, Kikuchi A, et al. Polysurgery of cell sheet grafts overcomes diffusion limits to produce thick, vascularized myocardial tissues. FASEB J 2006;20:708–10.
[51] Baar K, Birla R, Boluyt MO, Borschel GH, Arruda EM, Dennis RG. Self-organization of rat cardiac cells into contractile 3-D cardiac tissue. FASEB J 2005;19:275–7.